Theoretical Study of Ruthenium-Catalyzed Hydrogenation of Carbon Dioxide into Formic Acid. Reaction Mechanism Involving a New Type of σ-Bond Metathesis

Yasuo Musashi*,† and Shigeyoshi Sakaki*,‡

Contribution from the Information Processing Center, Kumamoto University, Kumamoto 860-8555, Japan, and Department of Applied Chemistry and Biochemistry, Faculty of Engineering, Kumamoto University, Kumamoto 860-8555, Japan

Received October 25, 1999

Abstract: Ruthenium-catalyzed hydrogenation of CO_2 into formic acid was theoretically investigated with the DFT(B3LYP) method, where *cis*-$RuH_2(PH_3)_4$ was adopted as a catalyst model. Theoretical calculations show that (1) CO_2 insertion into the Ru−H bond occurs with an activation energy (E_a) of 29.3 kcal/mol in *cis*-$RuH_2(PH_3)_4$ and with an E_a value of 10.3 kcal/mol in *cis*-$RuH_2(PH_3)_3$; (2) six-membered σ-bond metathesis of $RuH(\eta^1\text{-}OCOH)(PH_3)_3(H_2)$ occurs with a much smaller E_a value (8.2 kcal/mol) than four-membered σ-bond metathesis (E_a = 24.8 kcal/mol) and five-membered H−OCOH reductive elimination (E_a = 25.5 kcal/mol); (3) three-membered H−OCOH reductive elimination requires a very much larger E_a value of 43.2 kcal/mol; (4) if PH_3 dissociates from *cis*-$RuH_2(PH_3)_4$, the CO_2 hydrogenation takes place through the CO_2 insertion into the Ru−H bond of $RuH_2(PH_3)_3$ followed by the six-membered σ-bond metathesis, where the rate-determining step is the CO_2 insertion; and (5) if PH_3 does not dissociate from *cis*-$RuH_2(PH_3)_4$ and *cis*-$RuH(\eta^1\text{-}OCOH)(PH_3)_4$, the CO_2 hydrogenation proceeds through the CO_2 insertion into the Ru−H bond of *cis*-$RuH_2(PH_3)_4$ followed by the H−OCOH reductive elimination, where the rate-determining step is the CO_2 insertion. From the above conclusions, one might predict that (1) excess phosphine suppresses the reaction, (2) the use of solvent that facilitates phosphine dissociation is recommended, and (3) the ruthenium(II) complex with three phosphine ligands is expected to be a good catalyst. The electronic processes and characteristic features of the CO_2 insertion reaction and the σ-bond metathesis are discussed in detail.

1. Introduction

CO_2 fixation is an important subject of research in organometallic and catalytic chemistries.[1] One of the most attractive and interesting reactions of CO_2 fixation is transition metal catalyzed CO_2 hydrogenation into formic acid,[2−6] because formic acid is often used as a raw material in organic syntheses. Such transition metal complexes as $[WH(CO)_5]^-$,[7] $RhH(P\text{-}P)_2$ (P-P = 1,2-bis(diphenylphosphino)ethane or 1,3-bis(diphenylphosphino)propane),[8] $[RhH_2(PMe_2Ph)_3(L)]^+$ (L = H_2O or THF),[9] and *cis*-$RuH_2(PR_3)_4$ (R = Me[10] or Ph[11]) were used as catalysts of this reaction. Tsai and Nicholas experimentally investigated a hydrogenation reaction of CO_2 catalyzed by $[RhH_2(PMe_2Ph)_3(L)]^+$ and spectroscopically detected Rh(III) η^1-formate and Rh(III) η^2-formate complexes.[9] From these results, they proposed that the reaction proceeded through CO_2 insertion into the Rh(III)−H bond of $[RhH_2(PMe_2Ph)_3(L)]^+$ followed by reductive elimination of formic acid from $[RhH(\eta^1\text{-}OCOH)(PMe_2Ph)_3(L)]^+$ (L = solvent). Also, Leitner found that the Rh(I) hydride complex, RhH(P-P), catalyzed the hydrogenation of CO_2 into formic acid.[8] Later, Hutschka et al. experimentally and theoretically investigated this catalytic reaction in detail and proposed that this reaction took place through the CO_2 insertion into the Rh(I)−H bond of $RhH(PH_3)_2$ followed by the σ-bond metathesis of $Rh(\eta^1\text{-}OCOH)(PH_3)_2$ with molecular hydrogen.[12] Recently, Jessop, Ikariya, and Noyori succeeded in significantly efficient hydrogenation of CO_2 into formic acid with Ru(II) complexes in supercritical CO_2 (eq 1).[10] The extremely high

$$CO_2 + H_2 \xrightarrow[\text{in } scCO_2,\ N(C_2H_5)_3]{cis\text{-}RuH_2(PMe_3)_4} HCO_2H \qquad (1)$$

catalytic activity of the Ru(II) complex motivates us to investigate theoretically the Ru-catalyzed hydrogenation of CO_2 into formic acid, since it is considerably interesting and important to clarify the reaction mechanism and the rate-determining step of Ru(II)-catalyzed hydrogenation of CO_2.

In the present work, all the elementary steps involved in the catalytic cycle of Ru(II)-catalyzed hydrogenation of CO_2 into

† Information Processing Center.

‡ Department of Applied Chemistry and Biochemistry, Faculty of Engineering.

(1) Behr, A. *Carbon Dioxide Activation by Metal Complex*; VCH Publishers: Weinheim, Germany, 1988.

(2) Jessop, P. G.; Morris, R. H. *Coord. Chem. Rev.* **1992**, *121*, 155.

(3) Jessop, P. G.; Ikariya, T.; Noyori, R. *Chem. Rev.* **1995**, *95*, 259.

(4) (a) Leitner, W. *Angew. Chem., Int. Ed. Engl*. **1995**, *34*, 2207. (b) Leitner, W. *Coord. Chem. Rev*. **1996**, *153*, 257.

(5) Komiya, H.; Yoshida, Y.; Hirai, H. *Chem. Lett*. **1975**, 1223.

(6) Kröcher, O.; Köppel, R. A.; Baiker, A.*Chem. Commun*. **1997**, 453.

(7) Darensbourg, D. J.; Ovalles, C. *J. Am. Chem. Soc*. **1984**, *106*, 3750.

(8) Burgemeister, T.; Kastner, F.; Leitner, W. *Angew. Chem., Int. Ed. Engl*. **1993**, *22*, 739.

(9) Tsai, J.-C.; Nicholas, K. M. *J. Am. Chem. Soc*. **1992**, *114*, 5117.

(10) (a) Jessop, P. G.; Ikariya, T.; Noyori, R. *Nature* **1994**, *368*, 231. (b) Jessop, P. G.; Ikariya, T.; Noyori, R. *Science* **1995**, *269*, 1065. (c) Jessop, P. G.; Ikariya, T.; Noyori, R. *J. Am. Chem. Soc*. **1996**, *118*, 344.

(11) Inoue, Y.; Izumida, H.; Sasaki, Y.; Hashimoto, H. *Chem. Lett*. **1976**, 863.

(12) (a) Hutschka, F.; Dedieu, A.; Eichberger, M.; Fornika, R.; Leitner, W. *J. Am. Chem. Soc*. **1997**, *119*, 4432. (b) Hutschka, F.; Dedieu, A. *J. Chem. Soc., Dalton Trans*. **1997**, 1899.

10.1021/ja9938027 CCC: $19.00
Published on Web 04/08/2000

formic acid are theoretically investigated with the density functional theory (DFT) method. Our purposes here are (1) to elucidate the reaction mechanism, (2) to show what is the rate-determining step, and (3) to provide detailed knowledge of characteristic features of this reaction. Our intention here is to present a clear conclusion of the reaction mechanism and to indicate the importance of six-membered σ-bond metathesis of $RuH(\eta^1\text{-}OCOH)(PH_3)_n$ ($n = 3$ or 4) with H_2. This six-membered σ-bond metathesis is significantly different from the four-membered σ-bond metathesis proposed recently,[12] but similar to formate-assisted six-membered H_2 splitting which was previously proposed by Darensbourg et al.[7] in the hydrogenation of CO_2 into formic acid catalyzed by $[WH(CO)_5]^-$ but has received little attention so far. Similar H_2 splitting assisted by a ligand has also been reported by Morris et al.,[13] Crabtree et al.,[14] and Milet et al.[15]

2. Catalyst Model and Examined Reactions

Since a ruthenium(II) complex, $RuH_2(PMe_3)_4$, was used as a catalyst in Ru(II)-catalyzed hydrogenation of CO_2 into formic acid,[10] we adopted here *cis*-$RuH_2(PH_3)_4$ as a catalyst model. Komiya et al.[16] and Kolomnikov et al.[17] experimentally reported that the CO_2 insertion into the Ru−H bond of *cis*-$RuH_2(PR_3)_4$ (**1**) occurred with phosphine dissociation when PPh_3 was used as a ligand. On the other hand, Jessop et al. reported that addition of PMe_3 did not suppress the stoichiometric CO_2 insertion in *cis*-$RuH_2(PMe_3)_4$.[10c] This result suggests that CO_2 is inserted into the Ru−H bond without PMe_3 dissociation. Several reports suggested that a bulky phosphine tends to dissociate from the central metal.[18] Thus, we investigated two types of CO_2 insertion; one is the CO_2 insertion into the Ru−H bond of a six-coordinate Ru(II) complex, *cis*-$RuH_2(PH_3)_4$ (**1a**) (eq 2a), without PH_3 dissociation, and the other is the CO_2 insertion into the Ru−H bond of a five-coordinate Ru(II) complex, *cis*-$RuH_2(PH_3)_3$ (**1b**) (eq 2b), with PH_3 dissociation.

$$cis\text{-}RuH_2(PH_3)_4 + CO_2 \rightarrow RuH(\eta^1\text{-}OCOH)(PH_3)_4 \quad (2a)$$

$$cis\text{-}RuH_2(PH_3)_3 + CO_2 \rightarrow RuH(\eta^1\text{-}OCOH)(PH_3)_3 \quad (2b)$$

$$RuH(\eta^1\text{-}OCOH)(PH_3)_n \rightarrow Ru(PH_3)_n(HCOOH) \text{ or } Ru(PH_3)_4 + HCOOH \quad (n = 3 \text{ or } 4) \quad (3)$$

$$Ru(PH_3)_4(HCOOH) + H_2 \rightarrow cis\text{-}RuH_2(PH_3)_4 + HCOOH \quad (4)$$

$$Ru(PH_3)_4 + H_2 \rightarrow cis\text{-}RuH_2(PH_3)_4 \quad (5)$$

$$RuH(\eta^1\text{-}OCOH)(PH_3)_4 + H_2 \rightarrow cis\text{-}RuH(\eta^1\text{-}OCOH)(PH_3)_3(H_2) + PH_3 \rightarrow RuH_2(PH_3)_3(HCOOH) + PH_3 \quad (6a)[19]$$

$$RuH(\eta^1\text{-}OCOH)(PH_3)_3 + H_2 \rightarrow cis\text{-}RuH(\eta^1\text{-}OCOH)(PH_3)_3(H_2) \rightarrow RuH_2(PH_3)_3(HCOOH) \quad (6b)[19]$$

Two reaction courses are considered possible in the formation of formic acid from a formate complex, $RuH(\eta^1\text{-}OCOH)(PH_3)_n$ ($n = 3$ or 4); one is the reductive elimination of formic acid from $RuH(\eta^1\text{-}OCOH)(PH_3)_n$, to yield $Ru(PH_3)_n(HCOOH)$ (eq 3). In this case, the ruthenium dihydride complex of an active species must be reproduced through the oxidative addition of H_2 to a Ru(0) complex, $Ru(PH_3)_n(HCOOH)$ or $Ru(PH_3)_n$ (eqs 4 and 5). The other is the σ-bond metathesis of $RuH(\eta^1\text{-}OCOH)(PH_3)_n$ with a hydrogen molecule (eqs 6a and 6b). To perform the σ-bond metathesis, H_2 must coordinate with Ru. When $n = 4$, $RuH(\eta^1\text{-}OCOH)(PH_3)_4$ possesses no room for H_2 coordination, and therefore, substitution of H_2 for PH_3 must occur to yield $RuH(\eta^1\text{-}OCOH)(PH_3)_3(H_2)$, as shown in eq 6a. When $n = 3$, $RuH(\eta^1\text{-}OCOH)(PH_3)_3$ has an unoccupied coordination site, and therefore, H_2 easily coordinates with Ru to afford $RuH(\eta^1\text{-}OCOH)(PH_3)_3(H_2)$, as shown in eq 6b. We investigated here six-membered σ-bond metathesis and four-membered σ-bond metathesis in $RuH(\eta^1\text{-}OCOH)(PH_3)_3(H_2)$. When the σ-bond metathesis takes place, the active species of *cis*-$RuH_2(PH_3)_3$ is produced concomitantly with the formation of HCOOH, and therefore, the oxidative addition of H_2 to a Ru(0) complex does not need to occur.

3. Computations

The density functional theory (DFT) method[20] was employed here with the B3LYP functional for the exchange correlation term.[21,22] Geometries were optimized with the following basis set system (BS-I): core electrons of P (up to 2p) and Ru (up to 3d) were replaced with effective core potentials (ECPs), and their valence electrons were represented with (21/21/1) and (311/311/211) sets, respectively.[23,24] MIDI-4 sets[25] were employed for C and O, and a (4s)/[2s] set[26] was used for H. A d-polarization function[25] was added on C and O, and a p-polarization function[26] was added on the active hydrogen atom that was hydride and the H atom of formate. Energy changes[27] were calculated with a better basis set system (BS-II), using DFT(B3LYP)/BS-I optimized geometries. In BS-II, a (541/541/211)[28] set was employed for Ru with the same ECPs as those in BS-I.[24] A MIDI-4 set[25] was used for P, where a d-polarization function was added.[25] For C and O, (9s 5p 1d)/[3s 2p 1d] sets[26] were used with a p-diffuse function.[26] For the active H atom, a (5s 1p)/[3s 1p] set[29] was employed.

(13) (a) Park, S.; Ramachandran, R.; Lough, A. J.; Morris, R. H. *J. Chem. Soc., Chem. Commun*. **1994**, 2201. (b) Lough, A. J.; Park, S.; Ramachandran, R.; Morris, R. H. *J. Am. Chem. Soc*. **1994**, *116*, 8356.

(14) (a) Lee, J. C., Jr.; Rheingold, A. L.; Muller, B.; Pregosin, P. S.; Crabtree, R. H. *J. Chem. Soc., Chem. Comm*. **1994**, 1021. (b) Lee, J. C., Jr.; Peris, E.; Rheingold, A. L.; Crabtree, R. H. *J. Am. Chem. Soc*. **1994**, *116*, 11014. (c) Crabtree, R. H.; Siegbahn, P. E. M.; Eisenstein, O.; Rheingold, A. L.; Koetzle, T. F. *Acc. Chem. Res*. **1996**, *29*, 348.

(15) (a) Milet, A.; Dedieu, A.; Kapteijn, G.; van Koten, G. *Inorg. Chem*. **1997**, *36*, 3223. (b) Milet, A.; Dedieu, A.; Canty, A. J. *Organometallics* **1997**, *16*, 5331.

(16) (a) Komiya, S.; Yamamoto, A. *J. Organomet. Chem*. **1972**, *46*, C58. (b) Komiya, S.; Yamamoto, A. *Bull. Chem. Soc. Jpn*. **1976**, *49*, 784.

(17) Kolomnikov, I. S.; Gusev, A. I.; Aleksandrov, G. G.; Lobeeva, T. S.; Struchkov, Yu. T.; Vol'pin, M. E. *J. Organomet. Chem*. **1973**, *59*, 349.

(18) (a) Tolman, C. A. *Chem. Rev*. **1977**, *77*, 313. (b) Yamamoto, A. *Organotransition Metal Chemistry*; John Wiley & Sons Inc.: New York, 1986; Chapter 6, pp 195−304 and references therein. (c) Collman, J. P.; Hegedus, L. S.; Norton, J. R.; Finke, R. G. *Principles and Applications of Oragnotransition Metal Chemistry*; University Science Books: Mill Valley, CA, 1987; Chapter 3, pp 57−234 and references therein.

(19) The term "cis" represents here that the H_2 ligand takes a position cis to the η^1-OCOH ligand.

(20) Parr, R. G.; Yang, W. *Density-Functional Theory of Atoms and Molecules*; Oxford University Press: New York, 1989.

(21) (a) Becke, A. D. *Phys. Rev. A* **1988**, *38*, 3098. (b) Becke, A. D. *J. Chem. Phys*. **1993**, *98*, 1372. (c) Becke, A. D. *J. Chem. Phys*. **1993**, *98*, 5648.

(22) Lee, C.; Yang, W.; Parr, R. G. *Phys. Rev. B* **1988**, *37*, 785.

(23) Hay, P. J.; Wadt, W. R. *J. Chem. Phys*. **1985**, *82*, 299.

(24) Wadt, W. R.; Hay, P. J. *J. Chem. Phys*. **1985**, *82*, 284.

(25) Huzinaga, S.; Andzelm, J.; Klobukowski, M.; Radzio-Andzelm, E.; Sakai, Y.; Tatewaki, H. *Gaussian Basis Sets for Molecular Calculations*; Elsevier: Amsterdam, 1984.

(26) Dunning, T. H.; Hay, P. J. In *Methods of Electronic Structure Theory*; Schaefer, H. F., Ed.; Plenum: New York, 1977; p 1.

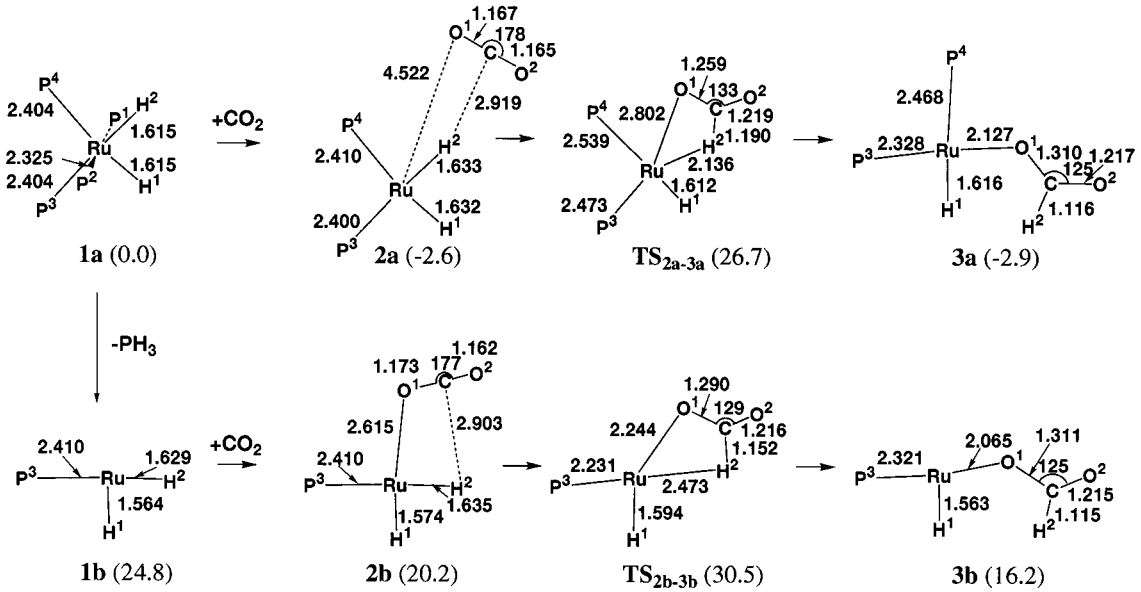

Figure 1. Geometry changes in the insertion of CO_2 into the Ru−H bond of *cis*-$RuH_2(PH_3)_n$ (n = 3 and 4). Bond distances are in angstroms and bond angles in degrees. In parentheses are the energy differences from **1a** (kcal/mol; DFT (B3LYP)/BS-II//DFT(B3LYP)/BS-I calculation). The P^1H_3 and P^2H_3 ligands, which are perpendicular to the P^3−Rh−H^1 plane, are omitted for brevity because the Ru−P^1 and Ru−P^2 distances hardly change through the hydrogenation of CO_2.

All the transition states were ascertained by vibrational frequency calculation with the DFT(B3LYP)/BS-I method. Gaussian 94 and 98 programs were used in these calculations.[30,31]

4. Results and Discussion

4.1. The CO_2 Insertion into the Ru−H Bond of $RuH_2(PH_3)_n$ (n = 3 or 4). Geometry changes in the CO_2 insertion reaction are shown in Figure 1. *cis*-$RuH_2(PH_3)_4$ **1a** takes a six-coordinate pseudo-octahedral structure. The optimized Ru−H bond distance (1.615 Å) is within a range of experimental values: 1.630 Å in $RuH(\eta^5\text{-}C_5H_5)(PMe_3)_2$ and 1.602 Å (average) in $[RuH_2(\eta^5\text{-}C_5H_5)(PMe_3)_2]^+$.[32] The similar Ru−H distance was previously reported in a theoretical investigation of $RuH_2(PH_3)_4$.[33] The Ru−P^1 and Ru−P^2 bonds are much longer than the Ru−P^3 and Ru−P^4 bonds because of the strong trans influence of the hydride ligand (see Figure 1 for P^1−P^4).

In the CO_2 insertion reaction without PH_3 dissociation, CO_2 approaches Ru to form a precursor complex, *cis*-$RuH_2(PH_3)_4(CO_2)$ **2a**. In **2a**, the Ru−H^2 bond (1.633 Å) and the Ru−P^4 bond (2.410 Å) are only 0.018 and 0.006 Å longer than those of **1a**, respectively, and the other moiety has almost the same geometry as that of **1a**. The CO_2 moiety also little distorts. The C−H^2 distance (2.919 Å) and the Ru−O^1 distance (4.522 Å) are quite long. Consistent with these features, the stabilization energy by CO_2 coordination is only 2.6 kcal/mol, as usually observed in the precursor complex of the CO_2 insertion into metal−hydride and metal−alkyl bonds.[8,34]

In the transition state $\mathbf{TS_{2a-3a}}$, only one imaginary frequency of 413i cm^{-1} was calculated. The eigenvector with this imaginary frequency mainly involves the approach of O^1 to Ru and the elimination of H^2 from Ru (See Supporting Information). These geometry changes are consistent with the CO_2 insertion into the Ru−H bond. In $\mathbf{TS_{2a-3a}}$, the Ru−H^2 bond considerably lengthens by 0.503 Å and the C−H^2 distance shortens to 1.190 Å, which is very close to the C−H bond of the formate anion. Also, the OCO angle significantly bends and both C−O bonds considerably lengthen. These features indicate that the Ru−H^2

(27) The reaction energy of hydrogenation of carbon dioxide into formic acid ($H_2 + CO_2 \rightarrow HCO_2H$) is calculated to be −5.4, −4.2, and −3.4 kcal/mol with the DFT(B3LYP), MP4(SDQ), and CCSD(T) methods, respectively, where the BS-II set was used. After correction of zero-point energy, the reaction energy is 2.2, 3.4, and 4.2 kcal/mol for DFT(B3LYP), MP4(SDQ), and CCSD(T) values, respectively, where the zero-point energy was evaluated with the DFT(B3LYP) method. The G2 calculation provides the reaction energy of 5.4 kcal/mol at 0 K. These results indicate that the DFT(B3LYP)/BS-II calculation tends to underestimate the endothermicity and that the zero-point energy correction increases the endothermicity. The zero-point energy is large when a molecule involves C−H and O−H bonds because these bonds exhibit high vibrational frequency. Thus, the CO_2 insertion would be slightly less exothermic and the H−OCOH reductive elimination would be slightly more endothermic than those calculated with the DFT(B3LYP)/BS-II method. However, this deviation would not change the conclusion about reaction courses because of considerably large differences in activation barrier between the four-membered σ-bond metathesis and the six-membered σ-bond metathesis and between the six-membered σ-bond metathesis and the five-membered H−OCOH reductive elimination.

(28) Couty, M.; Hall, M. B. *J. Comput. Chem.* **1996**, *17*, 1359.

(29) Clark, T.; Chandrasekhar, J.; Spitznagel, G. W.; Schleyer, P. v. R. *J. Comput. Chem.* **1983**, *4*, 294.

(30) Frisch, M. J.; Trucks, G. W.; Schlegel, H. B.; Gill, P. M. W.; Johnson, B. G.; Robb, M. A.; Cheeseman, J. R.; Keith, T. A.; Petersson, G. A.; Montgomery, J. A.; Raghavachari, K.; Al-Laham, M. A.; Zakrzewski, V. G.; Ortiz, J. V.; Foresman, J. B.; Cioslowski, J.; Stefanov, B. B.; Nanayakkara, A.; Challacombe, M.; Peng, C. Y.; Ayala, P. Y.; Chen, W.; Wong, M. W.; Andres, J. L.; Replogle, E. S.; Gomperts, R.; Martin, R. L.; Fox, D. J.; Binkley, J. S.; Defrees, D. J.; Baker, J.; Stewart, J. P.; Head-Gordon, M.; Gonzalez, C.; Pople, J. A. *GAUSSIAN 94*, revision E2; Gaussian Inc.: Pittsburgh, PA, 1995.

(31) Frisch, M. J.; Trucks, G. W.; Schlegel, H. B.; Scuseria, G. E.; Robb, M. A.; Cheeseman, J. R.; Zakrzewski, V. G.; Montgomery, J. A., Jr.; Stratmann, R. E.; Burant, J. C.; Dapprich, S.; Millam, J. M.; Daniels, A. D.; Kudin, K. N.; Strain, M. C.; Farkas, O.; Tomasi, J.; Barone, V.; Cossi, M.; Cammi, R.; Mennucci, B.; Pomelli, C.; Adamo, C.; Clifford, S.; Ochterski, J.; Petterson, G. A.; Ayala, P. Y.; Cui, Q.; Morokuma, K.; Malick, D. K.; Rabuck, A. D.; Raghavachari, K.; Foresman, J. B.; Cioslowski, J.; Ortiz, J. V.; Stefanov, B. B.; Liu, G.; Liashenko, A.; Piskorz, P.; Komaromi, I.; Gomperts, R.; Martin, R. L.; Fox, D. J.; Keith, T.; Al-Laham, M. A.; Peng, C. Y.; Nanayakkara, A.; Gonzalez, C.; Challacombe, M.; Gill, P. M. W.; Johnson, B. G.; Chen, W.; Wong, M. W.; Andres, J. L.; Gonzalez, C.; Head-Gordon, M.; Replogle, E. S.; Pople, J. A. *GAUSSIAN 98*, revision A6; Gaussian Inc.: Pittsburgh, PA, 1998.

(32) Brammer, L.; Klooster, W. T.; Lemke, F. R. *Organometallics* **1996**, *15*, 1721.

(33) Macgregor, S. A.; Eisenstein, O.; Whittlesey, M. K.; Perutz, R. N. *J. Chem. Soc., Dalton Trans.* **1998**, 291.

(34) Musashi, Y.; Sakaki, S. *J. Chem. Soc., Dalton Trans.* **1998**, 577.

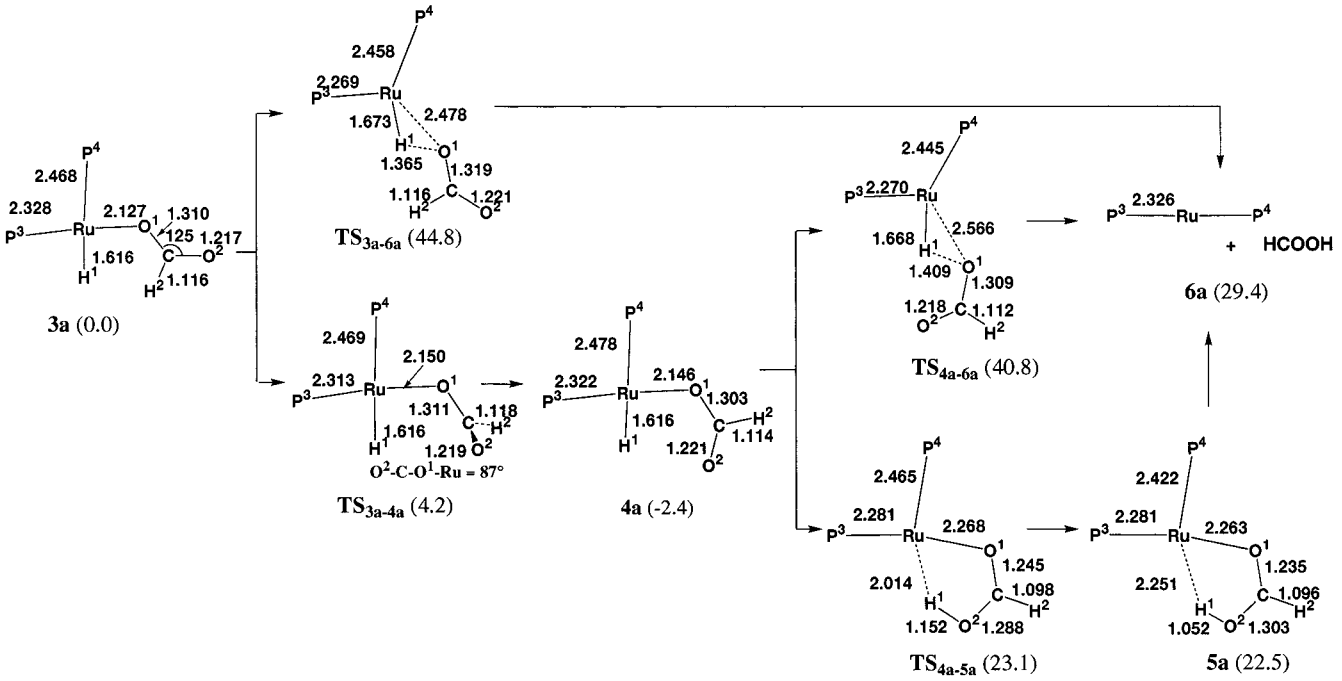

Figure 2. Geometry changes in the reductive elimination of formic acid from RuH(η^1-OCOH)$(PH_3)_4$ **3a**. Bond distances are in angstroms and bond angles in degrees. In parentheses are the energy differences from **3a** (kcal/mol; DFT(B3LYP)/BS-II//DFT(B3LYP)/BS-I calculation). The PH_3 ligands at a perpendicular position of the P^3-Rh-H^1 plane are omitted for brevity.

bond is much weakened and the formate anion has been almost formed at $\mathbf{TS_{2a-3a}}$. However, the $Ru-O^1$ distance (2.802 Å) is much longer than the usual Ru−formate bond, showing that the $Ru-O^1$ bond has not been sufficiently formed. This is because it is difficult for the Ru(II) complex to take a seven-coordinate structure and the $Ru-O^1$ bond cannot be formed without complete breaking of the Ru−H bond. As a result, a significantly high activation barrier (E_a = 29.3 kcal/mol) was calculated, where the E_a value is defined as an energy difference between $\mathbf{TS_{2a-3a}}$ and **2a**.

The insertion product **3a** is a monodentate formate complex which takes a six-coordinate pseudo-octahedral structure. Its $Ru-O^1$ distance (2.127 Å) is shorter than the experimental value reported for RuH(η^2-O_2CH)$(PPh_3)_3$,[17] probably because the $Ru-O^1$ bond of the monodentate formate complex is stronger than that of the bidentate formate complex, RuH(η^2-O_2CH)$(PPh_3)_3$.

PH_3 dissociation from *cis*-$RuH_2(PH_3)_4$ occurs with a destabilization energy of 24.8 kcal/mol to yield *cis*-$RuH_2(PH_3)_3$ **1b**. Though this destabilization energy is somewhat large, a bulky phosphine would dissociate from Ru(II) with a smaller destabilization energy.[18] CO_2 coordinates with **1b**, affording *cis*-$RuH_2(PH_3)_3(CO_2)$ **2b** with a stabilization energy of 4.6 kcal/mol. In **2b**, the $Ru-O^1$ and $C-H^2$ distances are rather long, being 2.615 and 2.903 Å, respectively. These geometrical features are similar to those of **2a**. In **2b**, CO_2 is inserted into the Ru−H bond through the transition state $\mathbf{TS_{2b-3b}}$, to yield a monodentate formate complex, RuH(η^1-OCOH)$(PH_3)_3$ **3b**. The eigenvector with an imaginary frequency (226i cm^{-1}) exhibits geometry changes consistent with the CO_2 insertion into the Ru−H bond. The geometrical features of $\mathbf{TS_{2b-3b}}$ resemble well those of $\mathbf{TS_{2a-3a}}$, except that the $Ru-P^3$ and $Ru-O^1$ bonds are significantly shorter than those of $\mathbf{TS_{2a-3a}}$. These shorter bonds would arise from the lesser steric repulsion between CO_2 and $RuH_2(PH_3)_3$ in $\mathbf{TS_{2b-3b}}$ than that in $\mathbf{TS_{2a-3a}}$. The activation energy was calculated to be 10.3 kcal/mol, which is much smaller than that for $\mathbf{TS_{2a-3a}}$. The insertion product **3b** takes a five-coordinate square-pyramidal structure, since Ru(II) takes a d^6 electron configuration. The Ru−(η^1-OCOH) moiety resembles well that of **3a**.

From these results, it is clearly concluded that CO_2 is inserted into the Ru−H bond with a large E_a value in *cis*-$RuH_2(PH_3)_4$ but with a small E_a value in *cis*-$RuH_2(PH_3)_3$.

4.2. Reductive Elimination of Formic Acid from RuH(η^1-OCOH)$(PH_3)_n$ (n = 3 or 4). RuH(η^1-OCOH)$(PH_3)_4$ **3a** and RuH(η^1-OCOH)$(PH_3)_3$ **3b** undergo the reductive elimination of formic acid (HCOOH), as shown in Figures 2 and 3, respectively. Starting from **3a**, the reductive elimination takes place through a three-membered transition state $\mathbf{TS_{3a-6a}}$ to afford Ru$(PH_3)_4$ + HCOOH **6a**. In $\mathbf{TS_{3a-6a}}$, only one imaginary frequency of 1118i cm^{-1} is calculated, and its eigenvector mainly involves the approach of H^1 to O^1. In this $\mathbf{TS_{3a-6a}}$, the $Ru-O^1$ bond considerably lengthens by 0.351 Å and the η^1-formate ligand significantly moves downward so that the O^1 atom approaches the H^1 atom. However, the $Ru-H^1$ bond little lengthens and the $O-H^1$ distance is still very long (1.673 Å). These features indicate that the $Ru-O^1$ bond much weakens but the $Ru-H^1$ bond has not been broken yet, and the new O−H bond formation has not been completed yet. In other words, the O^1-H^1 bond formation does not occur enough to compensate the energy destabilization by the $Ru-O^1$ bond weakening. As a result, the E_a value is very large (44.8 kcal/mol). In this reductive elimination, the product is considered to be $Ru(PH_3)_4$ + HCOOH **6a**, since the Ru(0) complex tends to take a four-coordinate structure. Further discussion of this reductive elimination is stopped here, because the reductive elimination more easily takes place via a different reaction course, as will be discussed below.

The η^1-formate complex **3a** isomerizes to **4a** by the rotation of η^1-formate about the $C-O^1$ bond, as shown in Scheme 1. In **4a**, the O^2 atom takes a position near the H^1 atom (see Scheme 1 for O^1, O^2, and H^1). This isomerization occurs via the transition state $\mathbf{TS_{3a-4a}}$. In $\mathbf{TS_{3a-4a}}$, only one imaginary frequency (164i cm^{-1}) is calculated, and its eigenvector mainly involves the rotation of the O^2CH^2 moiety about the $C-O^1$ bond. In this

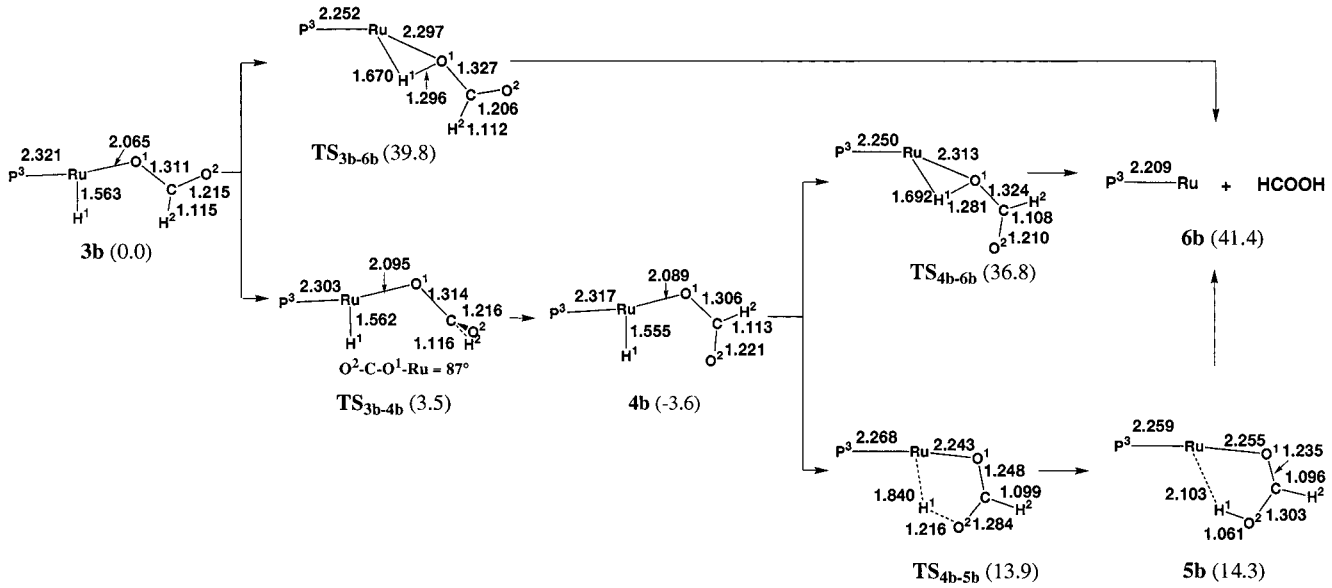

Figure 3. Geometry changes in the reductive elimination of formic acid from RuH(η^1-OCOH)(PH_3)$_3$ **3b**. Bond distances are in angstroms and bond angles in degrees. In parentheses are the energy differences from **3b** (kcal/mol; DFT(B3LYP)/BS-II//DFT(B3LYP)/BS-I calculation). The PH_3 ligands at a perpendicular position of the P^3-Rh-H^1 plane are omitted for brevity.

Scheme 1

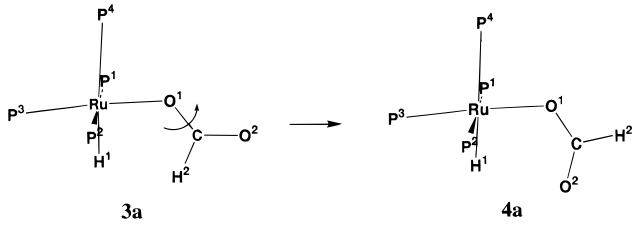

transition state, the dihedral angle between the $C-O^2-H^2$ and the $Ru-O^1-C$ planes is about 90°, while the geometry of the other part little changes. Consistent with the smalll geometry changes, the isomerization easily occurs with a much smaller E_a value of 6.6 kcal/mol.

From **4a**, two types of reductive elimination are considered to occur; one takes place through a three-membered transition state **TS$_{4a-6a}$** which needs a considerably large E_a value of 43.2 kcal/mol (the imaginary frequency of 1038i cm^{-1}). In this **TS$_{4a-6a}$**, $Ru-O^1$, O^1-H^1, and Ru−H distances are slightly longer than those of **TS$_{3a-6a}$**, while the geometry of the other moiety is almost the same as that of **TS$_{3a-4a}$**. The other type of reductive elimination proceeds through a five-membered transition state **TS$_{4a-5a}$** which needs a moderate E_a value of 25.5 kcal/mol (the imaginary frequency of 558i cm^{-1}). **TS$_{4a-5a}$** is considerably different from **TS$_{4a-6a}$**, as follows: (1) the $Ru-O^1$ distance moderately lengthens by 0.12 Å, indicating that the $Ru-O^1$ bond has not been broken yet; (2) the O^1 atom moderately moves downward; (3) the H^1 atom moderately moves toward the O^2 atom; and (4) the O^2-H^1 distance (1.152 Å) is close to the normal O−H bond of HCOOH. These features indicate that the H−O bond is easily formed in this **TS$_{4a-5a}$** with moderate geometry changes, unlike **TS$_{4a-6a}$**. As a result, the five-membered reductive elimination easily occurs through **TS$_{4a-5a}$** with a smaller E_a value than that of three-membered reductive elimination.

The product, Ru(PH_3)$_4$(HCOOH) **5a**, of this reductive elimination is a Ru(0) complex of HCOOH, which resembles well the transition state **TS$_{4a-5a}$**. Actually, **5a** is slightly more stable than **TS$_{4a-5a}$** by only 0.6 kcal/mol. The HCOOH dissociation from **5a** causes destabilization in energy by ca. 7 kcal/mol. This means that a Lewis base such as triethylamine is necessary to release formic acid from Ru, as experimentally known.[10]

Starting from RuH(η^1-OCOH)(PH_3)$_3$ **3b**, the reductive elimination of HCOOH also takes place through a three-membered transition state **TS$_{3b-6b}$**, as shown in Figure 3. In **TS$_{3b-6b}$**, the O^1 atom slightly moves downward from the Ru(PH_3)$_3$ plane and the H^1 atom considerably moves toward the O^1 atom. The geometry of the $Ru-O^1-H^1$ moiety resembles well those of **TS$_{3a-6a}$** and **TS$_{4a-6a}$**. Accordingly, the E_a value is very large (39.8 kcal/mol).

Also in **3b**, the η^1-formate ligand can rotate about the $Ru-O^1$ bond, to yield the isomer **4b** through the transition state **TS$_{3b-4b}$** like the isomerization of **3a** to **4a**. The formate complex **4b** undergoes the H−OCOH reductive elimination via either three-membered **TS$_{4b-6b}$** or five-membered **TS$_{4b-5b}$**. **TS$_{4b-6b}$** resembles well **TS$_{3b-6b}$**, and the E_a value is very large (40.4 kcal/mol). However, **TS$_{4b-5b}$** resembles **TS$_{4a-5a}$** and the E_a value is moderate (17.5 kcal/mol).

In the three-membered reductive elimination, the product, Ru(PH_3)$_3$ + HCOOH **6b**, is less stable than **TS$_{4b-6b}$**. This means that some product complex should exist between **TS$_{4b-6b}$** and **6a**. However, we omitted further examination, because this type of reductive elimination is not favorable and the five-membered reductive elimination occurs more easily. In the five-membered reductive elimination, the geometry of the product Ru(PH_3)$_3$(HCOOH) **5b** is similar to that of **TS$_{4b-5b}$**, and therefore, an energy difference between **TS$_{4b-5b}$** and **5b** is very small (only 0.4 kcal/mol). The HCOOH dissociation from **5b** gives rise to a destabilization energy of 27.1 kcal/mol, to yield Ru(PH_3)$_3$ + HCOOH **6b**, like **5a**. These results again indicate that Lewis base is necessary for this HCOOH dissociation.

4.3. Oxidative Addition of H_2 to Ru(PH_3)$_n$ (n = 3 or 4). Ru(PH_3)$_4$ **6a** and Ru(PH_3)$_3$ **6b** do not have a hydride ligand. Thus, the oxidative addition of H_2 to **6a** and **6b** (eq 5) must occur to form the active species *cis*-$RuH_2(PH_3)_n$ **1**. We investigated the H_2 oxidative addition but failed to optimize the geometry of the transition state. This reaction is significantly exothermic; the exothermicity (E_{exo}) is 31.9 and 38.1 kcal/mol for **1a** and **1b**, respectively. From these results, it is reasonably concluded that the oxidative addition of H_2 easily occurs with

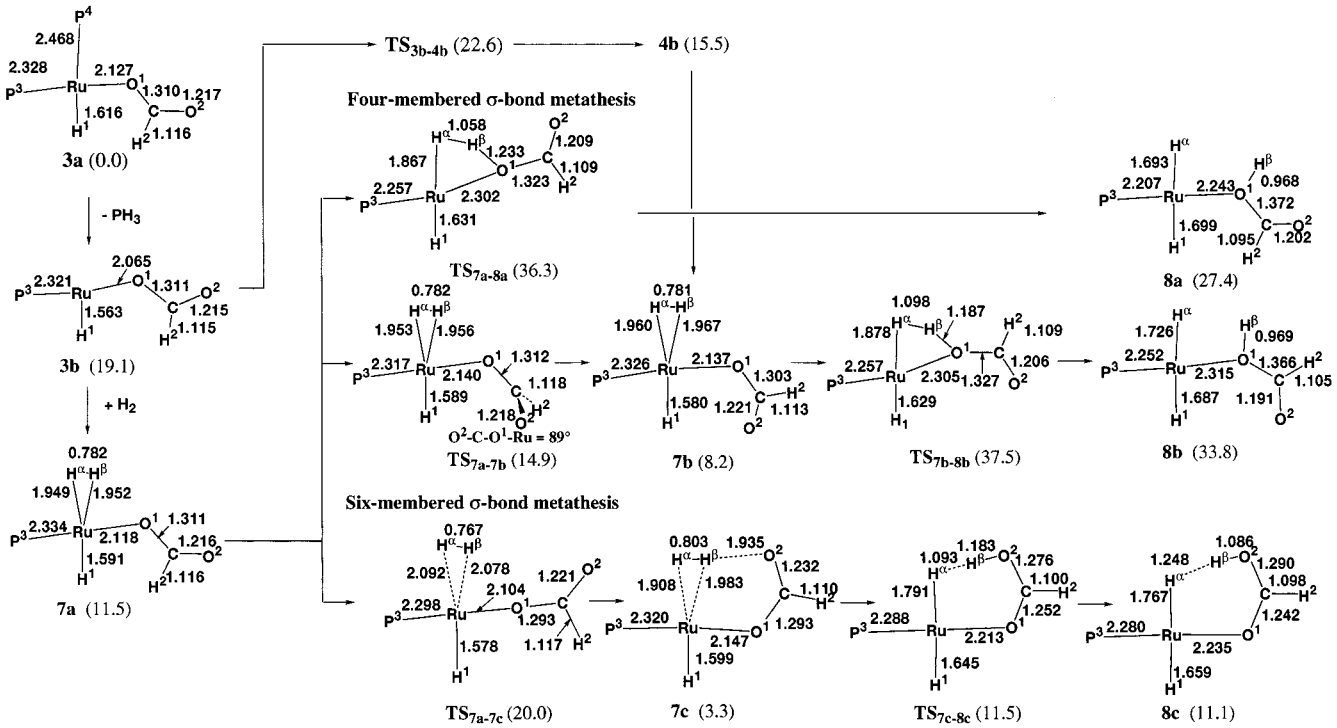

Figure 4. Geometry changes in the σ-bond metathesis of RuH(η^1-OCOH)$(PH_3)_3$ with H_2, in which H_2 is at a position trans to H^1. Bond distances are in angstroms and bond angles in degrees. In parentheses are the energy differences from **3a** (kcal/mol; DFT(B3LYP)/BS-II//DFT(B3LYP)/BS-I calculation). See Figure 3 for $\mathbf{TS_{3b-4b}}$ and **4b**. The PH_3 ligands at a perpendicular position of the P^3-Rh-H^1 plane are omitted for brevity.

no barrier. A similar result was theoretically reported in the oxidative addition of H_2 to $Ru(PH_3)_4$.[33] Moreover, the oxidative addition does not need to occur in the catalytic cycle, since the σ-bond metathesis of RuH(η^1-OCOH)$(PH_3)_n$ with H_2 more easily occurs than the reductive elimination and the active species is reproduced through the σ-bond metathesis, as will be discussed below. Thus, we stopped further investigation of this oxidative addition.

4.4. σ-Bond Metathesis of RuH(η^1-OCOH)$(PH_3)_n$ ($n = 3$ or 4) with H_2. In the σ-bond metathesis of RuH(η^1-OCOH)-$(PH_3)_4$ **3a** with H_2, PH_3 must be substituted for H_2, to yield RuH(η^1-OCOH)$(PH_3)_3(H_2)$. We failed to optimize the transition state of associative substitution of H_2 for PH_3, since one PH_3 dissociated from Ru during the geometry optimization of the transition state. This result suggests that the associative substitution of H_2 for PH_3 would not occur, probably because **3a** is coordinatively saturated and the seven-coordinate structure is very unstable in the Ru(II) complex. Thus, the dissociative substitution of H_2 for PH_3 was investigated here. The PH_3 dissociation gives rise to a destabilization energy of 19.1 kcal/mol to afford a coordinatively unsaturated complex RuH(η^1-OCOH)$(PH_3)_3$ **3b** (see Figure 4). This destabilization energy is smaller than the activation barrier of any reductive elimination of H−OCOH from **3a**, showing that the PH_3 dissociation occurs more easily than the H−OCOH reductive elimination.

H_2 coordinates with **3b**, to afford a molecular hydrogen complex, RuH(η^1-OCOH)$(PH_3)_3(H_2)$ **7a**, with a stabilization energy of 7.6 kcal/mol. In **7a**, the $H^\alpha-H^\beta$ bond distance (0.782 Å) is slightly longer than the normal H−H bond (see Figure 4 for H^α and H^β), and the geometry of the Ru(η^1-OCOH)$(PH_3)_3$ moiety is almost the same as that of **3a**, as shown in Figure 4. These features indicate that the $H^\alpha-H^\beta$ bond is little activated by Ru and the coordinate bond of H_2 is weak. Starting from **7a**, the four-membered σ-bond metathesis takes place through $\mathbf{TS_{7a-8a}}$ which exhibits only one imaginary frequency of 1252i cm^{-1}. The eigenvector with the imaginary frequency mainly involves the approach of H^β to O^1 but little involves the approach of H^α to Ru. The $H^\alpha-H^\beta$ bond lengthens by 0.276 Å, while the $Ru-H^\alpha$ and O^1-H^β distances are much longer than the normal Ru−H and O−H bond distances, respectively, showing that the new $Ru-H^\alpha$ and O^1-H^β bonds have not been completely formed at $\mathbf{TS_{7a-8a}}$. As a result, the E_a value is considerably large (24.8 kcal/mol). This four-membered σ-bond metathesis is similar to the previously reported four-membered σ-bond metathesis of Rh(η^1-OCOH)$(PH_3)_2$ with H_2[12a] and the H−H splitting by PdH(OH)(NH_3).[15a]

Isomerization of **7a** to **7b** easily proceeds via a transition state $\mathbf{TS_{7a-7b}}$ with a small activation barrier of only 3.4 kcal/mol (an imaginary frequency of 167i cm^{-1}). The σ-bond metathesis from **7b** also occurs through a four-membered transition state $\mathbf{TS_{7b-8b}}$ with a very large E_a value of 29.3 kcal/mol (an imaginary frequency of 1184i cm^{-1}).

The five-coordinate formate complex **4b**, which is discussed in Figure 3, also undergoes coordination of H_2 to yield **7b**, as shown in Figure 4. From **7b**, the four-membered σ-bond metathesis might occur through $\mathbf{TS_{7b-8b}}$. However, this reaction needs a considerably large E_a value (see above and Figure 4). Thus, the σ-bond metathesis starting from **4b** is ruled out here.

Also, **7a** isomerizes to **7c** through a transition state $\mathbf{TS_{7a-7c}}$, which needs an E_a of 8.5 kcal/mol. From **7c**, σ-bond metathesis proceeds through a six-membered transition state $\mathbf{TS_{7c-8c}}$ (Figure 4). The eigenvector with the imaginary frequency (764i cm^{-1}) mainly involves the approach of H^β to O^2 and that of H^α to Ru. In $\mathbf{TS_{7c-8c}}$, the $H^\alpha-H^\beta$ and $Ru-O^1$ distances lengthen by 0.290 and 0.066 Å, respectively, the $Ru-H^\alpha$ distance shortens by 0.117 Å, the $Ru-H^1$ bond lengthens by 0.046 Å, and the O^2-H^β distance shortens to 1.183 Å. These geometrical changes indicate that the $H^\alpha-H^\beta$ bond is considerably weakened and the new $Ru-H^\alpha$ and O^2-H^β bonds have been almost formed. The activation energy was calculated to be 8.2 kcal/mol, which is much less than those of the four-membered metathesis and the three-membered and five-membered reductive eliminations.

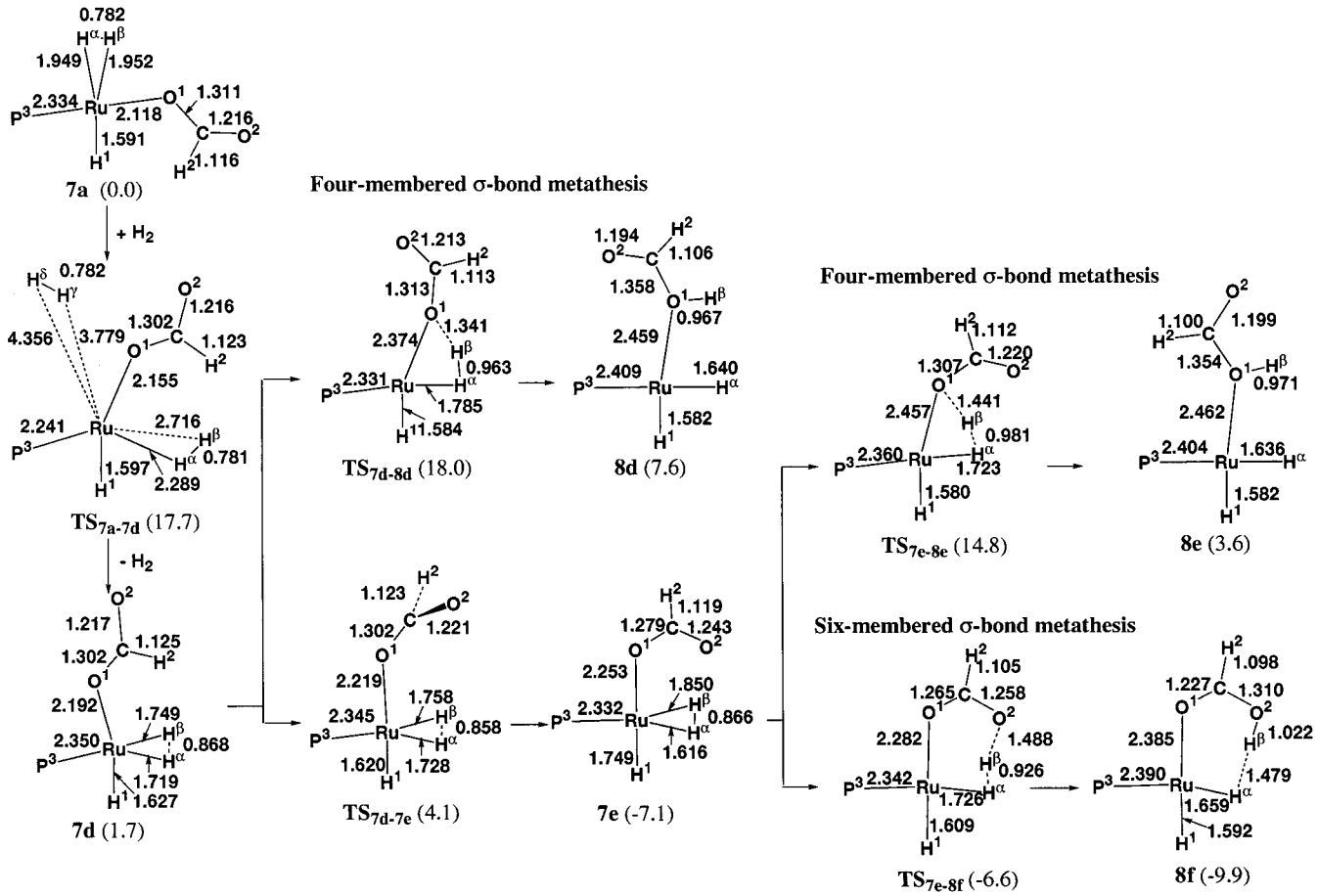

Figure 5. Geometry changes in the σ-bond metathesis of RuH(η^1-OCOH)$(PH_3)_3$ with H_2, in which H_2 is at a position cis to H^1. Bond distances are in angstroms and bond angles in degrees. In parentheses are the energy differences from **7a** (kcal/mol; DFT(B3LYP)/BS-II//DFT(B3LYP)/BS-I calculation). The PH_3 ligands at a perpendicular position of the P^3-Rh-H^1 plane are omitted for brevity.

From these results, it should be concluded that the six-membered σ-bond metathesis is the easiest reaction path to afford formic acid. Darensbourg and Ovalles previously suggested that the formation of formic acid might occur through either the formate-assisted heterolytic cleavage of H_2 or the reductive elimination of formic acids concomitant with the oxidative addition of H_2 to W.[7] The former reaction is essentially the same as the six-membered σ-bond metathesis presented here. Also, Morris et al.[13] and Crabtree et al.[14] experimentally proposed that the ligand-assisted H−H splitting occurred through a six-membered interaction, which is essentially the same as the present six-membered σ-bond metathesis. Milet et al.[15b] also theoretically investigated the ligand-assisted H−H splitting through a multimembered interaction which is similar to our six-membered σ-bond metathesis. The geometry of the product complex RuH-$(PH_3)_3$(HCOOH) **8c** is similar to that of $\mathbf{TS_{7c-8c}}$. Consistent with this result, **8c** is only 0.4 kcal/mol more stable than $\mathbf{TS_{7c-8c}}$ and less stable than **7c** by 7.8 kcal/mol.[35] Thus, the six-membered σ-bond metathesis via $\mathbf{TS_{7c-8c}}$ is endothermic and the reverse reaction easily occurs, which again indicates that Lewis base is necessary in the reaction.

In this σ-bond metathesis, the Ru−H^α bond is formed at a position trans to H^1 (hydride). This geometry is unfavorable because of the strong trans influence of the H ligand. Actually, the Ru−H^α bonds in $\mathbf{TS_{7c-8c}}$ and **8c** are much longer than the Ru−H bond of **3a**. This unfavorable situation disappeared if the σ-bond metathesis occurred in **7d** (Figure 5) in which the η^1-formate ligand is at a position trans to H^1. Thus, we investigated the isomerization of **7a** to **7d** followed by the σ-bond metathesis of **7d**, as shown in Figure 5. This isomerization occurs via $\mathbf{TS_{7a-7d}}$ with an E_a value of 17.7 kcal/mol. This isomerization corresponds to the associative substitution of $H^\alpha-H^\beta$ for $H^\gamma-H^\delta$. In $\mathbf{TS_{7a-7d}}$, the $H^\gamma-H^\delta$ moiety is much distant from Ru and it does not seem to interact with Ru. Only the approach of $H^\alpha-H^\beta$ to Ru is observed but the movement of $H^\gamma-H^\delta$ is not observed in the eigenvector with imaginary frequency (259i cm^{-1}). In **7d**, the $H^\alpha-H^\beta$ bond distance (0.868 Å) is much longer, the Ru−H_2 distance is much shorter, and the Ru−O^1 and Ru−H^1 bonds are longer than those of **7a**. These features show that H_2 more strongly and η^1-formate less strongly coordinates with Ru, which is interpreted in terms of a strong trans influence of H^1 in **7a** and **7d**. From **7d**, the four-membered σ-bond metathesis occurs through $\mathbf{TS_{7d-8d}}$ with an E_a value of 16.3 kcal/mol. Also, **7d** undergoes the isomerization followed by either four-membered ($\mathbf{TS_{7e-8e}}$) or six-membered ($\mathbf{TS_{7e-8f}}$) σ-bond metathesis with an E_a value of 21.9 or 0.5 kcal/mol, respectively (see Figure 5). The E_a value for the **7d** → **7e** isomerization is also very small (2.4 kcal/mol). Though both six-membered and four-membered σ-bond metatheses require a lower E_a value than those of **7a** as expected, the **7a** → **7d** isomerization requires a larger E_a value (17.7 kcal/mol) than the **7a** → **7c** isomerization (8.5 kcal/mol) followed by the six-membered σ-bond metathesis of **7c** (8.2 kcal/mol). From these results, it is clearly concluded that we can neglect the reaction course involving the **7a** → **7d** isomerization followed by σ-bond

(35) A similar feature was found in the reaction between dihydrido(quinoline-8-acyliminol)bis(triphenylphosphine)iridium(III) and H_2, in which the ligand-assisted H−H splitting and the ligand-assisted H−H coupling reversibly occur.

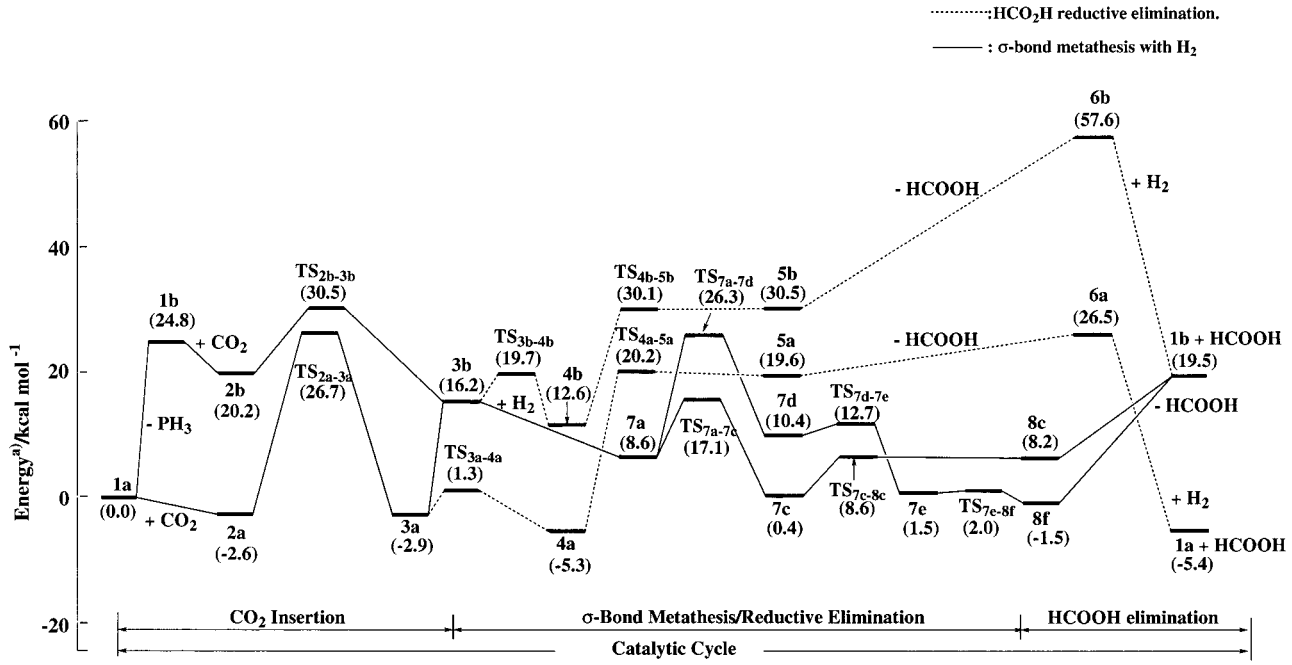

Figure 6. Energy changes in the $RuH_2(PH_3)_4$-catalyzed hydrogenation of CO_2 into formic acid. In parentheses are the energy differences from the sum of reactants (kcal/mol; DFT(B3LYP)/BS-II//DFT(B3LYP)/BS-I calculation).

metathesis, and that formic acid is produced through the **7a** → **7c** isomerization followed by the six-membered σ-bond metathesis via $\mathbf{TS_{7c-8c}}$.

4.5. Energy Changes in the Ru-Catalyzed Hydrogenation of CO_2 into Formic Acid. We have completed all the preparations to discuss energy changes along the $RuH_2(PH_3)_4$-catalyzed hydrogenation of CO_2 into formic acid.[36] Above results indicate that (1) the six-membered σ-bond metathesis is the easiest reaction course to yield formic acid from the ruthenium(II) formate complex, while the substitution of H_2 for PH_3 must occur to perform the σ-bond metathesis; and (2) if the substitution of H_2 for PH_3 cannot occur, not the σ-bond metathesis but the five-membered H−OCOH reductive elimination must take place as the last step. On the basis of these results, the following conclusions are presented about the reaction course: If PH_3 does not dissociate from Ru, the reaction proceeds through the CO_2 insertion into the Ru−H bond of *cis*-$RuH_2(PH_3)_4$ followed by the five-membered H−OCOH reductive elimination from $RuH(\eta^1\text{-OCOH})(PH_3)_4$; i.e., **1a** → **2a** → $\mathbf{TS_{2a-3a}}$ → **3a** → $\mathbf{TS_{3a-4a}}$ → **4a** → $\mathbf{TS_{4a-5a}}$ → **5a** → **6a** → **1a** + HCOOH, in which the rate-determining step is the CO_2 insertion (E_a = 29.3 kcal/mol), as shown in Figure 6. However, if PH_3 can dissociate from **3a**, the reaction mechanism changes. In this case, not the H−OCOH reductive elimination but the six-membered σ-bond metathesis takes place, since H_2 coordinates with Ru after PH_3 dissociation to afford $RuH(\eta^1\text{-OCOH})(PH_3)(H_2)$ and the six-membered σ-bond metathesis of this complex takes place with a smaller E_a value than the five-membered H−OCOH reductive elimination. As a result, the reaction proceeds through **1a** → **2a** → $\mathbf{TS_{2a-3a}}$ → **3a** → **3b** → **7a** → $\mathbf{TS_{7a-7c}}$ → **7c** → $\mathbf{TS_{7c-8c}}$ → **8c** → **1b** + HCOOH, in which the rate-determining step is also the CO_2 insertion (E_a = 29.4 kcal/mol) and the second largest barrier is the PH_3 dissociation in **3a** (19.1 kcal/mol). If PH_3 dissociates from **1a**, the catalytic reaction takes place through the CO_2 insertion into the Ru−H bond of *cis*-$RuH_2(PH_3)_3$ followed by the six-membered σ-bond metathesis; **1b** → **2b** → $\mathbf{TS_{2b-3b}}$ → **3b** → **7a** → $\mathbf{TS_{7a-7c}}$ → **7c** → $\mathbf{TS_{7c-8c}}$ → **8c**, in which the rate-determining step is the CO_2 insertion (E_a = 10.3 kcal/mol). From these results, it should be clearly concluded that if phosphine dissociates from Ru, this catalytic reaction easily proceeds. Actually, Jessop et al. experimentally reported that the addition of excess phosphine suppressed the reaction.[10] Thus, the use of solvent that facilitates phosphine dissociation is recommended. Also, the ruthenium(II) complex that has three phosphine ligands is expected to be a good catalyst.

4.6. Electronic Process of the CO_2 Insertion into the Ru(II)−H Bond. As described above, the CO_2 insertion into the Ru−H bond is the rate-determining step. Also, the six-membered σ-bond metathesis is of considerable importance, since the reaction course would be changed if this σ-bond metathesis was neglected. Thus, it is worthwhile to investigate electronic processes of these reactions. As shown in Figure 7, C atomic population considerably increases and O^1 and O^2 atomic populations moderately increase in both insertion reactions of **2a** and **2b**, while Ru atomic population significantly decreases in both, where natural bond orbital population was adopted.[37] However, H^2 atomic population little changes. These features suggest that the charge transfer to CO_2 from H^2 occurs considerably, and at the same time, H^2 is provided electrons from Ru, as shown in Scheme 2. The other important feature observed in Figure 7 is that the populations little change upon

(36) We estimated the activation energies of several important steps with the MP4(SDQ) method to examine if the DFT(B3LYP) method yields reliably the activation barrier. When the DFT(B3LYP) and MP4(SDQ) methods yielded considerably different values, we further calculated it with the CCSD(T) method. In the CO_2 insertion step (**2b** → $\mathbf{TS_{2b-3b}}$), the E_a value was calculated to be 10.3, 14.2, and 11.0 kcal/mol with DFT(B3LYP), MP4(SDQ), and CCSD(T) methods, respectively, showing that the DFT(B3LYP) value is similar to the CCSD(T) value. In the five-membered reductive elimination (**4b** → $\mathbf{TS_{4b-5b}}$), the E_a value was calculated to be 17.5 kcal/mol with the DFT(B3LYP) method and 16.0 kcal/mol with the MP4(SDQ) method. In the isomerization of **7a** to **7c**, the E_a value was calculated to be 8.5 kcal/mol with the DFT(B3LYP) method and 9.5 kcal/mol with the MP4(SDQ) method. In the six-membered σ-bond metathesis (**7c** → $\mathbf{TS_{7c-8c}}$), the E_a value was calculated to be 8.2 kcal/mol with the DFT(B3LYP) method and 9.3 kcal/mol with the MP4(SDQ) and CCSD(T) methods. These results suggest that the DFT(B3LYP) method, as well as MP4(SDQ) and CCSD(T) methods, provides a reliable activation barrier.

(37) Reed, A. E.; Curtiss, L. A.; Weinhold, F. *Chem. Rev.* **1988**, *88*, 899.

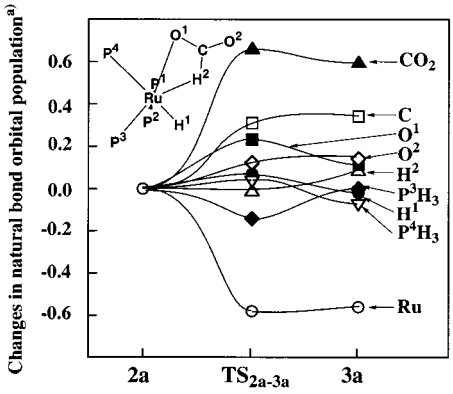

(A) CO_2 insertion in the six-coordinate *cis*-$RuH_2(PH_3)_4$

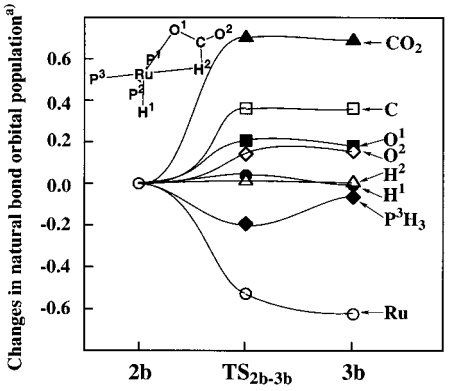

(B) CO_2 insertion in the five-coordinate *cis*-$RuH_2(PH_3)_3$

Figure 7. Population changes in the CO_2 insertion into the Ru−H bond of $RuH_2(PH_3)_n$ ($n = 3$ and 4): Natural bond orbital population[37] with DFT(B3LYP)/BS-II//DFT(B3LYP)/BS-I calculation. A positive value represents an increase in the population relative to the precursor complex.

Scheme 2

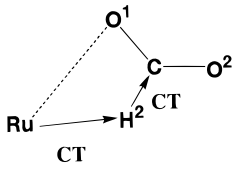

going to the product from the TS. This result clearly indicates that formate is almost formed at the TS, as displayed by geometry changes.

It is noted that O^1 atomic population increases at the TS but then decreases at the product in the insertion reaction of **2a**, while it little decreases at the product in the insertion reaction of **2b**. This difference suggests that the charge transfer from O^1 to Ru is difficult at $\mathbf{TS_{2a-3a}}$ in the insertion reaction of **2a**, probably because the O^1 atom cannot easily approach Ru due to the congested geometry of $\mathbf{TS_{2a-3a}}$ (see the geometry changes shown in Figure 1).

The orbital energy changes are compared between two insertion reactions, as shown in Figure 8. An important difference is that the HOMO becomes less stable upon going from **2a** to $\mathbf{TS_{2a-3a}}$ but becomes more stable upon going from **2b** to $\mathbf{TS_{2b-3b}}$. The next notable difference is that ϕ_{50} and ϕ_{51} significantly rise in energy upon going from **2a** to $\mathbf{TS_{2a-3a}}$, while ϕ_{41} and ϕ_{42} moderately rise in energy upon going from **2b** to $\mathbf{TS_{2b-3b}}$ (note that ϕ_{50} and ϕ_{51} of $\mathbf{TS_{2a-3a}}$ correspond to ϕ_{41} and ϕ_{42} of $\mathbf{TS_{2b-3b}}$, respectively). These differences are responsible for the larger E_a value of the insertion reaction of **2a**. Their contour maps are shown in Figure 8. In $\mathbf{TS_{2a-3a}}$, the HOMO involves considerable antibonding overlaps between Ru d and O p orbitals and between Ru d and H 1s orbitals. On the other hand, the HOMO of $\mathbf{TS_{2b-3b}}$ involves the antibonding overlap between Ru d and O p orbitals and nonbonding interaction between Ru d and H 1s orbitals. As a result, the HOMO of $\mathbf{TS_{2a-3a}}$ is much less stable than that of $\mathbf{TS_{2b-3b}}$. The next question is why the antibonding interaction between Ru d and H 1s orbitals is involved in $\mathbf{TS_{2a-3a}}$ but not in $\mathbf{TS_{2b-3b}}$. This would be interpreted in terms that the H^2 ligand is forced to take the position that suffers from the antibonding interaction with the Ru d orbital because of the congested structure of $\mathbf{TS_{2a-3a}}$. In $\mathbf{TS_{2b-3b}}$, CO_2 can take a better position, due to the less congested structure, and therefore, the reaction system can avoid the unfavorable situation in which H^2 gives rise to an antibonding overlap between Ru d and H 1s orbitals. The difference in behavior of molecular orbitals at lower energy is also understood in terms of the Ru−O^1 bonding interaction, as follows: ϕ_{50} and ϕ_{51} of $\mathbf{TS_{2a-3a}}$ involve weaker Ru−O^1 bonding than ϕ_{41} and ϕ_{42} of $\mathbf{TS_{2b-3b}}$, due to the longer Ru−O^1 distance in $\mathbf{TS_{2a-3a}}$ than that in $\mathbf{TS_{2b-3b}}$. The long Ru−O^1 distance in $\mathbf{TS_{2a-3a}}$ also arises from the congested structure.

4.7. Electronic Process of the σ-Bond Metathesis. In both six-membered and four-membered σ-bond metatheses, H^β atomic population significantly decreases, while H^α atomic population moderately increases, as shown in Figure 9. These population changes clearly show that both σ-bond metatheses occur through heterolytic bond cleavage of H−H. This feature is essentially the same as that of the ligand-assisted H_2 splitting in Ir(III) and Pd(II) complexes previously reported.[13−15]

Significant differences are observed between four-membered and six-membered σ-bond metatheses: the Ru atomic population gradually increases in the six-membered σ-bond metathesis, while it little increases at the TS but suddenly increases at the product in the four-membered σ-bond metathesis. Also, the O^1 atomic population increases at the TS and then decreases at the product in the four-membered σ-bond metathesis, while it little changes in the six-membered σ-bond metathesis. These features suggest that electron distribution smoothly changes in the six-membered σ-bond metathesis but it does not in the four-membered metathesis. This difference is interpreted in terms of orbital interaction, as follows: In the four-membered σ-bond metathesis, the O^1 lone pair orbital of formate must change its direction toward H^β to form the O−H bond, as shown in Scheme 3. This direction change weakens the CT interaction with Ru and decreases the Ru atomic population. Approach of formate to H_2 induces the polarization of the H_2 moiety so that the H^α atom becomes more negatively charged and the H^β atom becomes more positively charged. This polarization enhances the charge transfer from H^α to Ru. Thus, the Ru atomic population little changes at the TS, due to the compensation of these two CT interactions. At the product, the H^α ligand completely becomes hydride. Since the hydride ligand substantially donates electrons to Ru, the Ru atomic population considerably increases at the product. In the six-membered σ-bond metathesis, the situation is different; since the O^2 atom has a lone pair orbital which expands toward the H^β atom in **7c**, the O^2−H^β bond can be smoothly formed without considerable weakening of the Ru−O^1 bond in the six-membered σ-bond metathesis. Because of these smooth bond formations, the electron distribution smoothly changes in this σ-bond metathesis. The above discussion suggests that the O−H bond is more easily formed in the six-membered σ-bond metathesis than in the four-

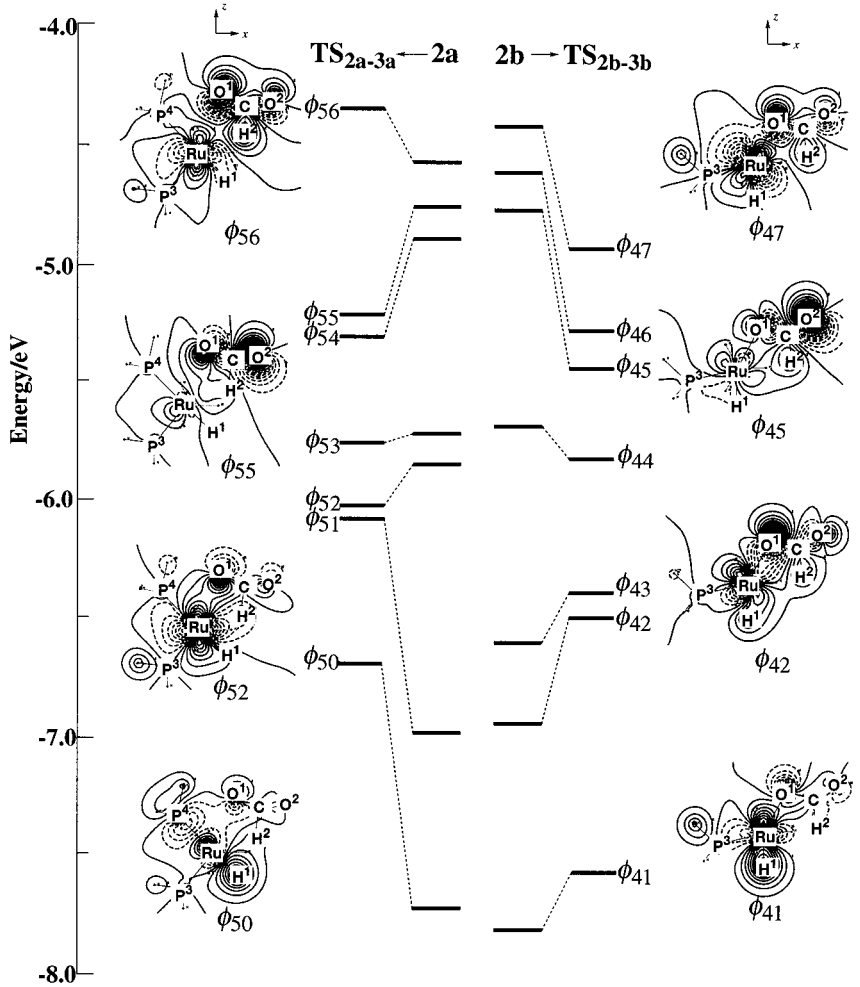

Figure 8. Energy levels and contour maps of several important molecular orbitals in the CO_2 insertion in *cis*-$RuH_2(PH_3)_n$ ($n = 3$ and 4): DFT(B3LYP)/BS-II//DFT(B3LYP)/BS-I calculation. Contour values are from -0.525 e·au^{-3} to 0.525 e·au^{-3} at intervals of 0.025 e·au^{-3}. Solid lines represent positive and zero contours, and dotted lines represent negative contours.

membered σ-bond metathesis. Actually, the formate moiety is more stable in **TS$_{7c-8c}$** than in **TS$_{7a-8a}$** by ca 10 kcal/mol, where the calculation was carried out for the formate anion whose geometry was taken to be the same as that in **TS$_{7a-8a}$** or **TS$_{7c-8c}$**. This energy difference roughly corresponds to the difference in E_a between six-membered and four-membered σ-bond metatheses. From these results, it is concluded that the six-membered σ-bond metathesis more easily takes place than the four-membered one because the O−H bond is more easily formed in the former than in the latter.

5. Conclusions

All of the possible elementary steps involved in ruthenium-catalyzed hydrogenation of CO_2 into formic acid were theoretically investigated with the DFT(B3LYP) method. Since *cis*-$RuH_2(PMe3)_4$ was experimentally used as a catalyst, we adopted *cis*-$RuH_2(PH_3)_4$ as a catalyst model. Important results are summarized, as follows: (1) the CO_2 insertion into the Ru−H bond occurs with difficulty in *cis*-$RuH_2(PH_3)_4$ but occurs easily in *cis*-$RuH_2(PH_3)_3$; (2) the H−OCOH reductive elimination requires a very large E_a value (40.3 and 44.8 kcal/mol for $n =$ 3 and 4, respectively) for the three-membered transition state but a moderately large E_a value (25.5 and 17.5 kcal/mol for n = 3 and 4, respectively) for the five-membered transition state; (3) though the four-membered σ-bond metathesis of *cis*-RuH-(η^1-OCOH)$(PH_3)_3(H_2)$ requires a very large E_a value (24.8 kcal/mol), the six-membered σ-bond metathesis occurs with a moderate E_a value (8.2 kcal/mol); and (4) the phosphine dissociation in *cis*-$RuH_2(PH_3)_4$ and *cis*-RuH(η^1-OCOH)$(PH_3)_4$ is necessary for the σ-bond metathesis.

From the above results, we can conclude that the reaction mechanism depends on the reaction conditions; when PH_3 cannot dissociate from Ru, the precursor complex for the σ-bond metathesis cannot be formed and only the H−OCOH reductive elimination can take place. Thus, the hydrogenation of CO_2 into formic acid takes place through the CO_2 insertion into the Ru−H bond of *cis*-$RuH_2(PH_3)_4$ followed by the H−OCOH reductive elimination, where the rate-determining step is the CO_2 insertion ($E_a = 29.3$ kcal/mol). When PH_3 can dissociate from Ru in *cis*-$RuH_2(PH_3)_4$, CO_2 is much more easily inserted into the Ru−H bond with a much smaller E_a value (10.3 kcal/mol), and the resultant complex, *cis*-RuH(η^1-OCOH)$(PH_3)_3$, easily undergoes the six-membered σ-bond metathesis with H_2, where the rate-determining step is the CO_2 insertion. Apparently, the PH_3 dissociation facilitates this catalytic reaction. Actually, it was experimentally reported that addition of excess PMe_3 suppressed the reaction.[10c]

From the above results, the use of solvent that facilitates phosphine dissociation is recommended in this catalytic reaction. Also, the Ru(II) complex that has three phosphine ligands is expected to be a good catalyst.

It should be noted that the six-membered σ-bond metathesis is the easiest reaction course to produce formic acid. If this σ-bond metathesis was neglected, the five-membered reductive

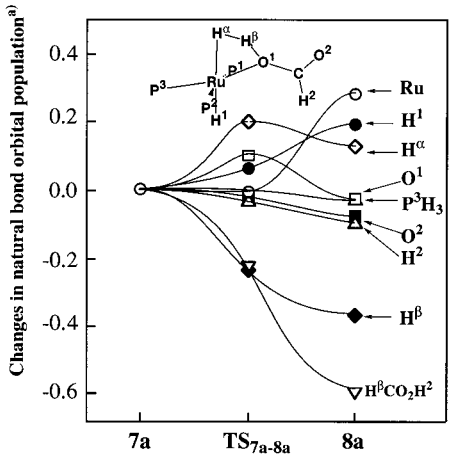

(A) Four-membered σ-bond metathesis

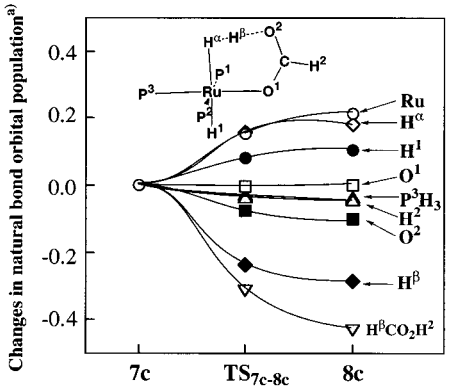

(B) Six-membered σ-bond metathesis

Figure 9. Population changes in the σ-bond metathesis of RuH(η^1-OCOH)$(PH_3)_3$ with H_2: Natural bond orbital population[37] with DFT(B3LYP)/BS-II//DFT(B3LYP)/BS-I calculation. A positive value represents an increase in the population relative to the H_2 complex.

elimination of H−OCOH became the easiest reaction to yield formic acid, since the five-membered reductive elimination needs a smaller E_a value (17.5 kcal/mol) than does the four-membered σ-bond metathesis (E_a = 24.8 kcal/mol). Thus, the neglect of the six-membered σ-bond metathesis leads to a different conclusion of the reaction mechanism, as follows: the CO_2 hydrogenation occurs through the CO_2 insertion into the Ru−H bond followed by the five-membered H−OCOH reductive elimination. This clearly shows the importance of the six-membered σ-bond metathesis. The six-membered σ-bond metathesis is essentially the same as the formate-assisted H_2 activation which was previously proposed by Darensbourg et al.[7] As discussed above, we should take the six-membered

Scheme 3

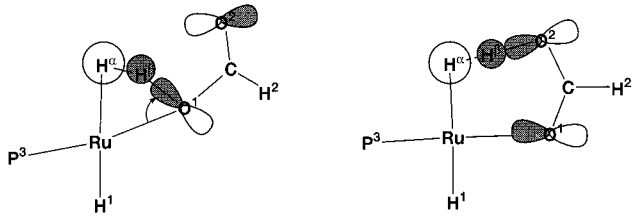

σ-bond metathesis into consideration when discussing the reaction mechanism of transition metal catalyzed hydrogenation of CO_2 into formic acid; for instance, the six-membered σ-bond metatheses of Rh(η^1-OCOH)$(PH_3)_2$ and [RhH(η^1-OCOH)$(PH_3)_3]^+$ occur with nearly no barrier.[38] The detailed investigation is in progress now.

Acknowledgment. All of the calculations were carried out with HP Exemplar Technical Server V2250KS of Information Processing Center of Kumamoto University and NEC-HPC of Institute for Molecular Science (Okazaki, Japan). This work was financially supported in part by the Grant-in-Aid for Scientific Research on Priority Areas (the Chemistry of Inter-Element of Linkage and the Molecular Physical Chemistry) from Ministry of Education, Culture, Sports and Science (284 and 403).

Supporting Information Available: Figures of the DFT(B3LYP)-optimized geometries and energy changes in the oxidative addition of H_2 to Ru$(PH_3)_n$ (n = 3 and 4), figures of the eigenvectors with imaginary frequency (DFT(B3LYP)/BS-I) in the transition states of the CO_2 insertion into the Ru−H bond of *cis*-Ru$H_2(PH_3)_n$ (n = 3 and 4), the reductive elimination of formic acid from RuH(η^1-OCOH)$(PH_3)_n$ (n = 3 and 4), the σ-bond metathesis of RuH(η^1-OCOH)$(PH_3)_3$ with H_2, and the isomerizations of **3a** → **4a**, **3b** → **4b**, **7a** → **7b**, **7a** → **7c**, **7a** → **7d**, and **7d** → **7e**. Energy levels of several important molecular orbitals for **2a**, **2b**, **7a**, **7c**, **TS$_{2a-3a}$**, **TS$_{2b-3b}$**, **TS$_{7a-8a}$**, and **TS$_{7c-8c}$** and their contour maps (PDF). This material is available free of charge via the Internet at http://pubs.acs.org.

JA9938027

(38) This six-membered σ-bond metathesis was not investigated in the theoretical work of Rh(I)-catalyzed hydrogenation of CO_2 into formic acid.[12] We investigated the six-membered σ-bond metatheses of Rh(η^1-OCOH)$(PH_3)_2$ and [RhH(η^1-OCOH)$(PH_3)_3]^+$ with H_2 and found that these reactions much more easily occurred with nearly no barrier than the four-membered σ-bond metathesis. These results suggest that Rh(I)-catalyzed hydrogenation of CO_2 into formic acid occurs with nearly no barrier and the six-membered bond metathesis of the formate complex should be taken into consideration when discussing the reaction mechanism of rhodium(I)- and rhodium(III)-catalyzed hydrogenations of CO_2 into formic acid.